Measurement and Characterization of the Time Variation of Indoor and Outdoor MIMO Channels at 2.4 and 5.2 GHz

Jon W. Wallace and Michael A. Jensen
Department of Electrical and Computer Engineering
Brigham Young University, 459 CB, Provo, UT, USA
E-mail: wall@ieee.org, jensen@ee.byu.edu

***Abstract*— The extent of time variation of measured multiple-input multiple-output (MIMO) wireless channels is explored. A prototype MIMO channel sounder developed at Brigham Young University, capable of probing 8×8 MIMO channels from 2-8 GHz with up to 100 MHz of instantaneous bandwidth, is used to measure representative indoor and outdoor scenarios at 2.4 and 5.2 GHz. New metrics are proposed to quantify the time variation observed in the channel measurements: eigenvalue level crossing rate, eigenvalue fade duration, rate of eigenvector angular deviation, and temporal capacity degradation. Two different models are used to fit the measurements: (1) a simple random matrix model and (2) a physical time-varying cluster model. The performance of these models is assessed in terms of their ability to reproduce the measured time-variation metrics.**

I. Introduction

With perfect channel state information (CSI) at the receiver and/or transmitter, theoretical studies and measurements have confirmed that multiple-input multiple-output (MIMO) wireless systems exhibit a large capacity improvement over their single-input single-output (SISO) counterparts. In real systems, however, where the MIMO channel is time variant, CSI is either imperfect or unavailable, leading to severe reductions in the available capacity. Therefore, the degree of channel time variation strongly impacts the target applications of MIMO techniques, the types of modulation/training employed, the number of transmit and receive antennas used, etc. Although previous studies have analyzed the effects of MIMO channel time variation, very little work exists that characterizes the extent of time variation in measured MIMO channels.

In this paper, we present a framework for the characterization of time variation in MIMO channels, based on wideband 8×8 MIMO channel measurements taken at Brigham Young University (BYU) in indoor and outdoor environments. The paper introduces a number of metrics that are useful for assessing the severity of time variation: eigenvalue level crossing rate, eigenvalue fade duration, rate of eigenvector angular deviation, and temporal capacity degradation. Finally, we investigate the ability of two different time-varying models to capture key behaviors observed in the measured MIMO channels: (1) a simple random matrix model and (2) an advanced time-variant physical clustering model. Due to space constraints, this paper focuses on our indoor channel measurements, with outdoor measurements to be included in a later publication.

II. Measurement System

Figure 1 depicts a block diagram of the wideband 8×8 MIMO channel sounder developed at BYU. At the transmit side, an arbitrary waveform generator creates a multi-tone signal with up to 100 MHz of instantaneous bandwidth, which is up-converted to an RF carrier in the range of 2-8 GHz, power amplified, and fed to an 8-way microwave switch connected to the transmit array. At the receive side, an 8-way switch routes signals from the array to a common RF receiver, consisting of low noise amplification, down-conversion, automatic gain control (AGC), and up to 500-MS/s PC-based A/D conversion. Control of the microwave switches is accomplished by a flexible synchronization unit that scans all possible antenna combinations, where the number of antennas and dwell time are selectable.

The receive waveforms and AGC levels are stored on a PC, allowing channel estimation to be performed off-line. The number of back-to-back channel snapshots that can be acquired is limited by the memory depth (512 MB) and sample rate (12.5-500 MS/s) of the A/D card. A "multiple record" feature allows delays to be placed between channel snapshots, thus extending the acquisition length. The number of locations probed in a single campaign is limited by hard drive space on the PC, where 100 GB can hold about 200 locations. Highly stable 10 MHz rubidium time/frequency references provide system synchronization at transmit and receive.

Antenna arrays at transmit and receive were 8-element uniform circular arrays, consisting of omnidirectional monopole elements with $\lambda/2$ inter-element spacing. Such arrays measure multipath from 360° of azimuthal view with a single channel snapshot, allowing the general characteristics of multipath and its time-variant behavior to be investigated.

MIMO channel time variation was studied by placing the transmitter in a fixed position and moving the receiver at a constant speed over a prescribed path of up to 4.5 m. The transmit signal consisted of 80 tones with 1 MHz separation, an antenna dwell time of 50 μS, and a center frequency of either 2.55 or 5.2 GHz. The 2.55 GHz center frequency was chosen instead of 2.45 GHz to avoid interfering with our existing WLAN network. Channels were acquired either back-to-back every 3.2 ms (fast mode) or with multiple record every 25.6 ms (slow mode), allowing both small- and large-scale variations to be investigated.

III. Measurement Scenarios

For the indoor scenario, depicted in Figure 2, the transmitter was stationary in a hallway, while the receiver was placed in 8 different rooms, thus simulating a reasonable WLAN topology. In each room, four different measurements were performed: (1) an acquisition with the transmitter turned off and the receiver stationary to assess the impact of co-channel interference, (2) a measurement with the receiver stationary to assess time variation from people/equipment, and measurements with the receiver moving at 0.3 m/s with either (3) fast, or (4) slow acquisition. Acquisition for case (1) with the transmitter off showed response only for the 2.55 GHz band, and this

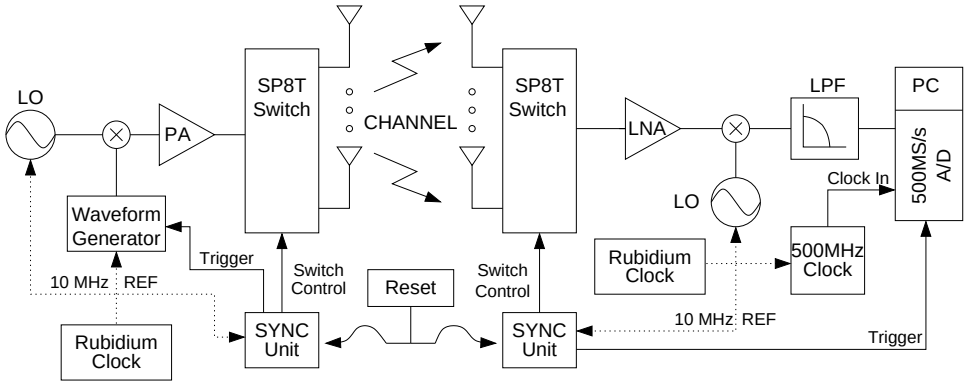

Fig. 1. Simplified block diagram of the 8×8 wideband MIMO channel sounder used to measure time variation of indoor and outdoor MIMO channels

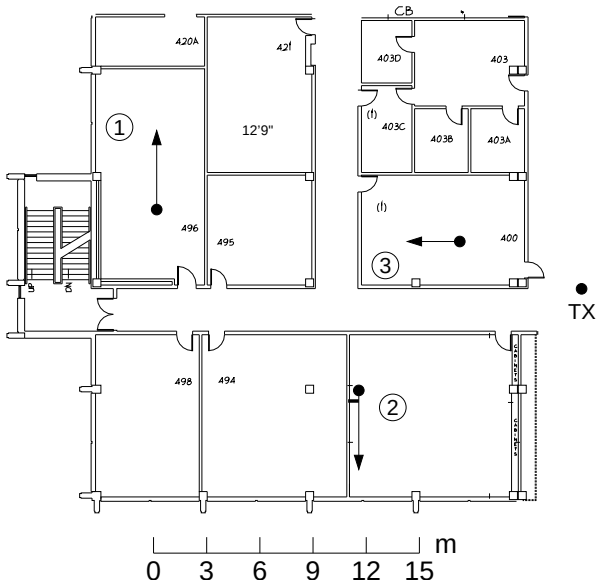

Fig. 2. Indoor measurement scenario for Locations 1-3, where other locations were in similar rooms to the right of the transmitter.

interference was negligible. Stationary receiver measurements produced a maximum Doppler of less than 1 Hz, which was small compared to the Doppler for moving measurements (10-20 Hz). Finally, inspection of the fast acquisition waveforms indicated that the slow acquisition channel sample rate was sufficient to capture the channel time variation. In the results that follow, only measurements from case (4) are considered.

IV. MIMO Time-variation Metrics

Key to this work are a set of metrics that indicate the degree of time variability of measured channels. Our goal in defining these metrics is not only to allow various measured channels to be classified, but also to assess the accuracy of time-varying models and to provide a connection between MIMO channel variation and the performance of other communications layers. Although our metrics are intended for *time*-varying channels, we characterize variation versus distance, allowing the results to be scaled for different movement speeds.

A. Eigenvalue Level Crossing Rate and Average Fade Duration

The singular value decomposition (SVD) of a single channel matrix $\mathbf{H}$ is given by $\mathbf{H} = \mathbf{USV}^H$, where $\mathbf{U} = [\mathbf{u}_1\mathbf{u}_2\ldots]$ and $\mathbf{V} = [\mathbf{v}_1\mathbf{v}_2\ldots]$ are the matrices of left and right singular vectors, and $\mathbf{S}$ is the diagonal matrix of ordered singular values. We refer to $\sigma_i(\mathbf{H}) = S_{ii}^2$ as the ith channel eigenvalue and column vectors $\mathbf{u}_i$ and $\mathbf{v}_i$ as the ith receive and transmit eigenvectors, respectively. Since σ_i represents a power gain, we can apply the standard single-antenna metrics to each eigenvalue.

Eigenvalue level crossing rate for the ith eigenvalue (ELCR_i) is computed as the number of times that $\sigma_i(\mathbf{H})$ drops below a specified threshold divided by the distance traveled. Eigenvalue average fade duration (EAFD_i) is the average fraction of path distance that the waveform lies below the threshold. The threshold will depend on the application, and in this work we use 2 dB below the mean.

ELCR and EAFD are interesting for multiple communications layers. For example, these values indicate how quickly a sophisticated MIMO physical layer (PHY) and medium access later (MAC) would need to adapt modulation and transmission rate to the time-varying channel quality. For constant rate/modulation transmission, they indicate the type of precoding required to overcome channel fades.

B. Eigenvector Angular Deviation

Eigenvector angular deviation (EAD) quantifies how quickly the transmit and receive eigenvectors rotate in complex M-dimensional space, where M is the number of antenna elements. We define EAD as

$$\theta_k = \frac{1}{N-k}\sum_{n=1}^{N-k}\cos^{-1}|\mathbf{v}^{(n)H}\mathbf{v}^{(n+k)}|, \qquad (1)$$

where k is the distance between two channel snapshots, N is the total number of snapshots, $\mathbf{v}^{(n)}$ is the nth snapshot of a given left or right singular vector, and $\{\cdot\}^H$ is the Hermitian operator.

EAD directly impacts how quickly a spatial multiplexing PHY must adapt its transmit/receive weights.

C. Capacity Degradation

Although the eigenchannel metrics are useful for system specification and design, they do not indicate the loss of channel quality in an information theoretic sense. To this end, we define a simple metric for quantifying capacity loss for a time-varying channel.

First, consider the case of *transmit CSI degradation* (TCD) where the receiver has perfect CSI but the transmitter only has

the delayed channel estimate $\hat{\mathbf{H}}$. We may define capacity for delayed transmit CSI as

$$C_T = \log_2 \left| \frac{\mathbf{H}\mathbf{Q}(\hat{\mathbf{H}})\mathbf{H}^H}{\sigma^2} + \mathbf{I} \right|, \tag{2}$$

where $\mathbf{H}$ is the true channel, σ^2 is the receiver noise variance, $\mathbf{Q}(\hat{\mathbf{H}})$ is the optimal transmit covariance given by the water-filling solution (assuming $\mathbf{H} = \hat{\mathbf{H}}$), $\mathbf{I}$ is the identity matrix, $\mathrm{Tr}\{\mathbf{Q}\} \leq P_T$, and P_T is total transmit power. In the results that follow, P_T and σ^2 are chosen such that the average SISO SNR is 10 dB. As the estimate $\hat{\mathbf{H}}$ becomes increasingly outdated, C_T will tend to decrease. At some distance, when the delayed capacity drops below the uninformed transmit capacity (C_T with $\mathbf{Q} = \mathbf{I}$), the transmit CSI is no longer useful, and we call this distance d_T.

Next, consider the case of *receive CSI degradation* (RCD), where both transmit and receive have outdated CSI. With perfect CSI, parallel channels may be formed by taking the SVD of the channel matrix, where the transmitter uses the right singular vectors $\mathbf{V}$ as transmit weights and the receiver uses the left singular vectors $\mathbf{U}$ as receive weights. The capacity of a such a system is

$$C = \max_{\mathbf{p}} \sum_i \log_2(1 + p_i S_{ii}/\sigma^2), \tag{3}$$

where the p_i are found according to water-filling. Imperfect estimates of the channel $\hat{\mathbf{H}} = \hat{\mathbf{U}}\hat{\mathbf{S}}\hat{\mathbf{V}}^H$ cause "cross-talk" among these parallel channels. Since we make no assumptions about the distribution of $\mathbf{H}$, we consider the worst case where the interference is i.i.d. Gaussian, resulting in a new mutual information of

$$C_R = \sum_i \log_2(1 + p_i S_{ii}/q_i), \tag{4}$$

where

$$q_i = \left\{\mathbf{M}\mathbf{P}\mathbf{M}^H\right\}_{ii} + \sigma^2 \tag{5}$$

$$\mathbf{M} = \hat{\mathbf{U}}^H\mathbf{H}\hat{\mathbf{V}} - \mathbf{\Phi}\hat{\mathbf{S}}, \tag{6}$$

$\mathbf{P} = \mathrm{diag}(\mathbf{p})$, and $\mathbf{\Phi}$ is a complex diagonal matrix whose diagonal elements have unit magnitude. In this work, we assume $\arg(\Phi_{ii}) = \arg(\{\hat{\mathbf{U}}^H\mathbf{H}\hat{\mathbf{V}}\}_{ii})$, thus masking the effect of average phase variations of the individual eigenchannels and focusing on the changing spatial structure. We refer to the point at which C_R drops to 50% of its maximum value as the distance d_R.

Typically, the transmit and receive degradation metrics are averaged over a number of different realizations: different starting points (training positions), multiple frequency bins, etc. This averaging provides a global picture of the effect of the time variation.

V. Time-variant MIMO Channel Models

Since accurate models are critical for the design and analysis of MIMO architectures, we investigate two different modeling strategies for time-variant MIMO channels: (1) a random matrix model following the multivariate complex normal (MVCN) distribution and (2) a time-variant clustering (TVC) model.

A. MVCN Model

We represent the complex gain from the jth transmitter to the ith receiver at time index n for a single frequency bin as $H_{ij}^{(n)}$. If these gains follow a (possibly time-varying) MVCN distribution in both time and space, the spatio-temporal variation of the MIMO channel is completely characterized by the multivariate mean ($\mathbf{M}$) and covariance ($\mathbf{R}$), or

$$M_{ij}^{(n)} = \mathrm{E}\left\{H_{ij}^{(n)}\right\} \tag{7}$$

$$R_{ij,k\ell}^{(n,m)} = \mathrm{E}\left\{(H_{ij}^{(n)} - M_{ij}^{(n)})(H_{k\ell}^{(n+m)} - M_{k\ell}^{(n+m)})^*\right\}, \tag{8}$$

where $\mathrm{E}\{\cdot\}$ is expectation. For a stationary distribution, $\mathbf{M}$ and $\mathbf{R}$ are not a function of n and can be obtained with sample averages. The difficulty of extracting these parameters from a nonstationary process depends on the severity of the nonstationarity, and may even be impossible for overspread processes [1]. Here, we consider a process characterized by a mean and covariance that vary slowly in time, allowing estimation by weighted sample averages, or

$$\begin{aligned} \hat{M}_{ij}^{(n)} &= \sum_{s=-\infty}^{\infty} w_s H_{ij}^{(s)} \\ \hat{R}_{ij,k\ell}^{(n,m)} &= \sum_{s=-\infty}^{\infty} w_{s+m/2} Z_{ij}^{(n+s)} Z_{k\ell}^{(n+s+m)*}, \end{aligned} \tag{9}$$

where $Z_{ij}^{(n)} = H_{ij}^{(n)} - \hat{M}_{ij}^{(n)}$, w is the weighting window, and the index $s + m/2$ is chosen to apply a weight of w_0 when the points $n+s$ and $n+s+m$ are equidistant from the center estimation point n.

The choice of the weighting window is a tradeoff between the bias and variance of the estimator. Here, we apply an exponential window, of the form $w_s = \exp(-|s/\ell_c|)$, where ℓ_c is the correlation length. If the process is determined to be nearly stationary over N_s samples, faithful estimates can be obtained with $4\ell_c = Ns$.

To determine a suitable value for ℓ_c, three different tests for multivariate normality were applied to the data: (1) Mardia's tests for multivariate skewness and (2) kurtosis [2], and (3) the Henze-Zirkler test [3]. Since previous results suggest that MIMO channels with large numbers of antennas do not strictly follow a multivariate normal distribution [4], we restrict our tests to 2×2 subsets of the MIMO data. Figure 3 depicts the average rejection rates for a significance level of 5% and a varying record length (sample size) for Locations 1-8 at 2.55 GHz. Very similar plots are obtained for 5.2 GHz. The results indicate that over distances of $4-8\lambda$ the rejection rates are acceptable, and we therefore let $\ell_c = 2\lambda$.

Once the time-varying mean and covariance have been estimated from the data via (9), we require a way of generating simulated channels. One approach involves forming $\mathbf{R}$ into a covariance matrix, computing the matrix square root, and using the result to correlate the elements of i.i.d. complex normal vectors. This approach is numerically prohibitive, however, since for 8 transmitters and receivers and 500 time steps, the covariance matrix has dimensions $32,000\times32,000$. A natural way to reduce this complexity is to assume that the covariance is separable in the time and space dimensions or $R_{ij,k\ell}^{(n,m)} = R_{S,ij,k\ell}^{(n)} R_T^{(n,m)}$. In this case, we need only find the matrix square root of a 500×500 matrix. For this separable

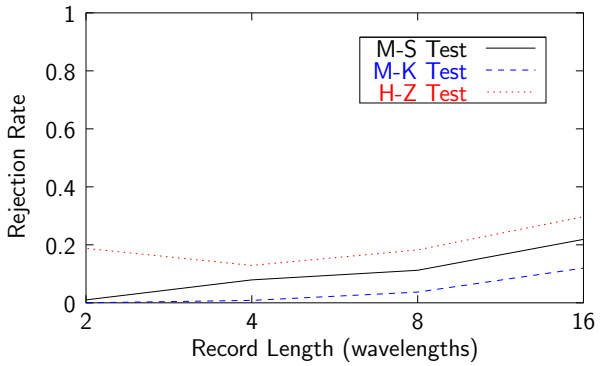

Fig. 3. Average rejection rates for three multivariate normal tests for Locations 1-8 at 2.55 GHz.

case, synthetic channels are generated stepwise as

$$B_{ij}^{(n)} = \sum_{n'} X_{T,nn'} A_{ij}^{(n')} \tag{10}$$

$$H_{ij}^{(n)} = \sum_{i'j'} X_{S,ij,i'j'}^{(n)} B_{i'j'}^{(n)}, \tag{11}$$

where $\mathbf{X}_T = \mathbf{R}_T'^{1/2}$, $\mathbf{X}_R = \mathbf{R}_S^{(n)1/2}$, $R'_{T,nn'} = R_T^{(n,n'-n)}$, i and j are stacked when used as a covariance index, and $A_{ij}^{(n')}$ are matrices of i.i.d. complex normal elements.

A nice feature of the MVCN model is that its parameters are directly extracted from the measured data. The main drawback, however, is the large number of parameters required to specify the distribution. Also, little physical insight is obtained from these parameters.

B. TVC Model

Another modeling approach for the time-varying MIMO channel is an extension of the cluster modeling strategy described in [5]. In this variant, we first obtain the double-directional Bartlett spatial spectrum for time step n as

$$P^{(n)}(\Omega) = \mathbf{b}^H(\Omega)\mathbf{R}_S^{(n)}\mathbf{b}(\Omega), \tag{12}$$

where $\Omega = (\phi_T, \phi_R)$, $b_{ik}(\Omega) = \psi_{R,i}(\phi_R)\ \psi_{T,k}(\phi_T)$ is the joint steering vector with $\psi_{S,i}(\phi_S) = \exp[j2\pi(x_{S,i}\cos\phi_S + y_{S,i}\sin\phi_S)]$, S is either T or R for transmit or receive, ϕ_S is azimuth angle, and x_i and y_i are x and y coordinates of the ith antenna. Given a true diffuse arrival power spectrum of $A(\Omega)$, the covariance is

$$\mathbf{R} = \int d\Omega A(\Omega)\mathbf{\Psi}(\Omega), \tag{13}$$

where $\mathbf{\Psi}(\Omega) = \mathbf{\Psi}_T(\phi_T) \otimes \mathbf{\Psi}_R(\phi_R)$ and $\mathbf{\Psi}_S(\phi_S) = \boldsymbol{\psi}_S(\phi_S)\boldsymbol{\psi}_S(\phi_S)^H$. Decomposing the true spectrum into basis functions (clusters) $A_p(\Omega)$, we have

$$A(\Omega) = \sum_p a_p A_p(\Omega), \tag{14}$$

and the Bartlett spectrum becomes

$$P^{(n)}(\Omega) = W[A] = \int d\Omega' A(\Omega')\mathbf{b}^H(\Omega)\mathbf{\Psi}(\Omega')\mathbf{b}(\Omega) \tag{15}$$

$$= \sum_p a_p W[A_p]. \tag{16}$$

By discretizing functions of the continuous variable Ω and matching left and right hand sides at a number of discrete points, we obtain the matrix equation $\mathbf{p} = \mathbf{W}\mathbf{a}$, which can solved via linear programming for the basis coefficients a_p. The main advantages of using the Bartlett spectrum, rather than operating on the covariance directly, are (1) the resulting equations are real, and (2) covariance structure representing non-propagating (evanescent) modes is removed.

In this work, we assume a set of Gaussian-shaped basis functions (clusters) with possible arrival angles of $\{0°, 5°, 10°, ..., 355°\}$ and angular spreads of $\{5°, 10°, 20°, 40°\}$. The time-variant nature of the clusters is obtained by estimating the basis coefficients from the time average of the measured Bartlett spectra, keeping the dominant basis functions (collectively representing 90% of the power spectrum), and estimating the optimal coefficients at each time step for this fixed basis. Because the initial double-directional estimate with the full basis can be very costly, we reduce the dimensionality by applying a single-directional version of the method to the average transmit and receive spectra individually, thus allowing a smaller set of important basis functions to be retained.

Synthetic channels are generated by assuming L rays per cluster, and computing the channel response as

$$H_{ij}^{(n)} = L^{-1/2} \sum_{p,\ell} a_p^{(n)1/2} \beta_{p\ell}\ \psi_{R,i}(\phi_{R,p\ell})\ \psi_{T,j}(\phi_{T,p\ell}), \tag{17}$$

where $\phi_{S,p\ell} \sim \mathcal{N}(\overline{\phi}_{S,p}, \sigma_{S,p}^2)$, $\beta_{p\ell} \sim \mathcal{CN}(0,1)$, $\overline{\phi}_{S,p}$ and $\sigma_{S,p}^2$ are the mean and variance of the departures/arrivals for cluster p, and $\mathcal{N}(\mu,\sigma^2)$ and $\mathcal{CN}(\mu,\sigma^2)$ are the real and complex normal distributions with mean μ and variance σ^2, respectively. Extensions to the model include allowing a different number of rays (richness) in each cluster, rays that dynamically appear or disappear in time, a time-variant set of clusters, etc. For this work, a fixed set of $L = 50$ rays per cluster is assumed for a each realization of the model. Also, note that this current model only attempts to fit the channel covariance, and has no provision for including non-fading components (channel mean).

Figure 4 plots an example double-directional spectrum estimate for Location 1 at 2.55 GHz.

C. Model Comparisons

To demonstrate the ability of the specified models to capture the time-variant characteristics of MIMO channels, we apply the proposed time-variation metrics directly to measured data as well as synthetic channels generated with the MVCN and TVC models. When computing covariance, mean, and time-variation metrics from data, we consider 8 frequency bins separated by 10 MHz as statistically independent realizations, thus creating an effectively larger sample size. For the models at each location, 10 independent temporal evolutions (realizations) are considered.

Figure 5 shows a typical result for the RCD capacity metric (4), taken from Location 5 at 5.2 GHz. In most cases, the RCD capacity for the MVCN model dropped too quickly and the TVC model provided a better fit. On the other hand, the MVCN model matched TCD capacity very well. This result is not surprising, however, since the RCD capacity depends on the small scale variations, which may not be captured very well by forcing separability of time and space. TCD capacity, on the other hand, is governed only by the long term spatial statistics, which will be matched almost exactly by MVCN.

Table I lists the metrics applied to measured data and synthetic channels at 2.55 and 5.2 GHz, where all metrics

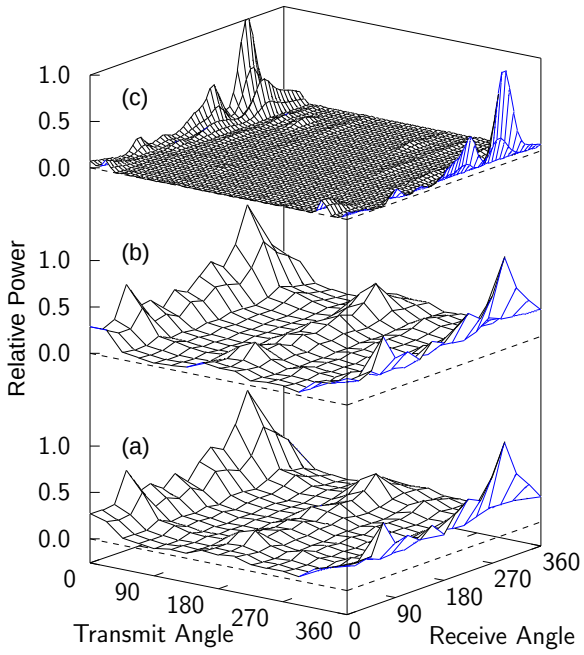

Fig. 4. Example time-average spatial spectrum estimate for Location 1 at 2.55 GHz: (a) measured and (b) modeled Bartlett spatial spectra and (c) estimated true spectrum.

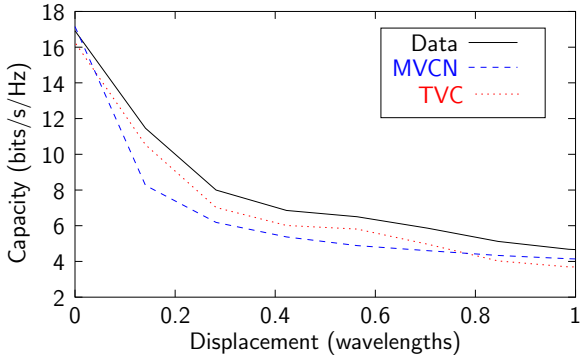

Fig. 5. Typical RCD capacity plot taken from Location 5 at 5.2 GHz.

are in terms of wavelengths λ, and σ is average absolute deviation from measured values. Although the TVC model better predicts metrics associated with short-term variations (C_R, d_R, ELCR, and EAFD), the MVCN model more faithfully captures the long-term behavior (C_T and d_T).

VI. Conclusion

Although MIMO systems exhibit high capacity with perfect CSI, imperfect CSI can lead to reductions in available capacity. This paper provided a number of metrics for characterizing the time variation of MIMO channels, useful for classifying channels, assessing modeling accuracy, and connecting time variation to the performance of higher communications layers. The metrics were applied to measured 8×8 indoor channels at 2.55 and 5.2 GHz to demonstrate their utility. A random matrix model based on the MVCN distribution and a cluster model both showed promise in capturing the key behaviors of the time-varying channels. Later work will demonstrate the application of these metrics and models to outdoor data, where similar conclusions may be drawn, although the scales of time variation are generally longer due to less multipath. Also, future work is needed to produce models that can accurately predict all metrics with relatively few parameters.

TABLE I
Comparison of Metrics for Indoor Data/Models

(a) 2.55 GHz

	d_R (λ)			d_T (λ)		
Loc.	Data	MVCN	TVC	Data	MVCN	TVC
1	0.28	0.14	0.21	7.8	6.1	$\geq$ 30.0
2	0.28	0.14	0.28	17.5	6.7	$\geq$ 30.0
3	0.21	0.14	0.14	1.7	0.3	13.5
4	0.21	0.14	0.21	3.2	1.5	12.6
5	0.21	0.14	0.21	7.2	6.2	$\geq$ 20.0
6	0.21	0.14	0.21	$\geq$ 20.0	$\geq$ 20.0	$\geq$ 20.0
7	0.21	0.14	0.21	2.0	0.3	26.8
8	0.21	0.14	0.21	3.0	1.1	32.7
σ	-	0.09	0.02	-	2.5	15.4
	ELCR_1 ($1/\lambda$)			ELCR_2 ($1/\lambda$)		
Loc.	Data	MVCN	TVC	Data	MVCN	TVC
1	0.31	0.83	0.37	0.40	0.96	0.42
2	1.21	1.42	0.39	1.05	1.57	0.47
3	0.81	1.17	0.55	0.52	1.09	0.56
4	0.58	0.83	0.37	0.67	0.86	0.44
5	0.76	0.99	0.44	0.47	1.11	0.52
6	0.40	0.77	0.32	0.56	0.98	0.46
7	0.33	0.71	0.30	0.44	0.69	0.33
8	0.72	0.89	0.43	0.56	1.11	0.56
σ	-	0.31	0.26	-	0.46	0.14

(b) 5.2 GHz

	d_R (λ)			d_T (λ)		
Loc.	Data	MVCN	TVC	Data	MVCN	TVC
1	0.28	0.28	0.28	39.6	35.5	$\geq$ 70.0
2	0.28	0.28	0.28	28.5	23.1	33.0
3	0.28	0.14	0.14	3.4	1.5	19.7
4	0.28	0.14	0.70	18.3	18.6	44.9
5	0.28	0.14	0.28	27.3	27.6	30.1
6	0.28	0.14	0.28	$\geq$ 50.0	47.5	$\geq$ 50.0
7	0.28	0.28	0.28	27.8	14.5	$\geq$ 70.0
8	0.28	0.14	0.14	25.5	21.3	$\geq$ 70.0
σ	-	0.09	0.09	-	4.0	20.9
	ELCR_1 ($1/\lambda$)			ELCR_2 ($1/\lambda$)		
Loc.	Data	MVCN	TVC	Data	MVCN	TVC
1	0.25	0.61	0.25	0.35	0.71	0.29
2	0.25	0.58	0.32	0.42	0.69	0.49
3	0.22	0.60	0.54	0.57	0.74	0.51
4	0.41	0.57	0.29	0.56	0.72	0.43
5	0.25	0.63	0.20	0.41	0.70	0.46
6	0.42	0.70	0.32	0.47	0.76	0.37
7	0.20	0.69	0.29	0.31	0.49	0.37
8	0.43	0.65	0.45	0.51	0.85	0.50
σ	-	0.32	0.10	-	0.26	0.07

Acknowledgment

This work was supported in part by the National Science Foundation under Information Technology Research Grants CCR-0313056 and CCF-0428004 and in part by the US Army Research Office under the Multi-University Research Initiative (MURI) Grant # W911NF-04-1-0224.

References

[1] G. Matz, "A time-frequency calculus for time-varying systems and nonstationary processes with applications," Ph.D. dissertation, Technische Universität Wien, 2000.
[2] K. V. Mardia, J. T. Kent, and J. M. Bibby, *Multivariate analysis*. Academic Press, 1979.
[3] N. Henze and B. Zirkler, "A class of invariant consistent tests for multivariate normality," *Commun. Statist.-Theor. Meth.*, vol. 19, no. 10, pp. 3595–3618, 1990.
[4] T. Svantesson and J. W. Wallace, "Tests for assessing multivariate normality and the covariance structure of MIMO data," in *Proc. 2003 IEEE Intl. Conf. Acoustics, Speech, and Signal Processing*, vol. 4, Hong Kong, Apr. 6-10, 2003, pp. 656–659.
[5] J. Wallace, H. Özcelik, M. Herdin, E. Bonek, and M. Jensen, "A diffuse multipath spectrum estimation technique for directional channel modeling," in *Proc. 2004 IEEE Intl. Conf. Commun.*, vol. 6, Paris, France, Jun. 20-24 2004, pp. 3183–3187.